

M. J. Jiang · D. Harris · H.-S. Yu

## A novel approach to examining double-shearing type models for granular materials

Received: 25 August 2004 / Published online: 4 May 2005  
© Springer-Verlag 2005

**Abstract** A novel method, designated as the Rotation of Principal Axes Method (RPAM), capable of examining the double-shearing type kinematic models for granular materials is presented herein. A planar velocity field, which is proposed to represent a continuous rotation of principal strain rate axes, is applied to each model to analyse the rotation of principal stress axes. The proposed approach was proven to show main features of the double-shearing model, the double-sliding free-rotating model, and the revised double-shearing model, in a simple way interesting to geo-researchers. Furthermore, the RPAM was efficient in investigating the choice of a Cosserat rotation rate in kinematic theories and determining a key model parameter in the revised double-shearing model.

**Keywords** Examination approach · Double-shearing type models · Granular materials · Rotation of principal axes method · Kinematics

### 1 Introduction

The double-shearing type kinematic models for granular materials are a kind of physically-established plasticity models that describe ‘fully-developed’ plane plastic flow of granular materials by means of kinematic theories, in which the deformation is usually postulated to occur by shear along stress/velocity characteristics [1–8]. As emphasized by Spencer [9]: the constitutive equation is actually a relation between three tensors: stress, strain rate and stress rate. Hence, these theories are in essence able to capture one of most complicated behaviours of granular materials that cannot be properly

described using classical plasticity, i.e. non-coaxiality (the non-coincidence of the principal stress tensor and the principal plastic deformation-rate tensor), which is one of very important and interesting topics in geo-research [10]. Compared to several advanced non-coaxial constitutive models in modern geomechanics, e.g. hypo-plastic models [11, 12] and multi-laminate models [13, 14], one of salient advantages of these kinematic theories is that the models are physically established in a simple formulation, in the case of planar deformation, with a pair of kinematic equations governing the velocity field.

However, only a few of examination works have been carried out upon these theories, and as will be shown in the next section the exhibited aspects are either distant from the main concerns in geotechnical community or clarified by some unconventional experimental, theoretical or numerical technique. Hence, the kinematic models, although they have several salient advantages, are not as popular as other advanced and complicated non-coaxial constitutive models in geotechnical community. Moreover, there seems not to be obvious criterion for examining the kinematic models. As stated by Collins [15], ‘one unsatisfactory aspect of these theories is that at the present time there is not obvious criterion for preferring one of these various models to any of the others of this type.’ This constitutes one of the strong motivations for this study.

In this paper, after briefly introducing current examination methods, a novel approach, referred to as the Rotation of Principal Axes Method (RPAM), is proposed to examine the double-shearing type kinematic models for granular materials. By using the proposed method, the main features of several kinematic models are highlighted. In addition are discussed the possibility of choosing a Cosserat rotation rate in kinematic theories and the way of determining a key parameter in a kinematic model, by using the RPAM.

### 2 Current examination methods

The kinematic models for granular material flow were firstly developed by de Josselin de Jong [1], then by Spencer [2]. A

M. J. Jiang (✉) · H.-S. Yu  
Nottingham Centre for Geomechanics,  
School of Civil Engineering, University of Nottingham,  
Nottingham, NG7 2RD, UK  
E-mail: mingjing.jiang@nottingham.ac.uk  
Fax: +44-115-951-3898  
Tel.: +44-115-951-3938

M. J. Jiang · D. Harris  
School of Mathematics,  
University of Manchester,  
Manchester, M60 1QD, UK

similar model had been previously proposed by Mandel [3]. de Josselin de Jong [4] called his model the double-sliding free-rotating model and Spencer called his model the double-shearing model. These theories were originally developed for incompressible, rigid-plastic flow of granular materials, and were then extended to a class of ideal dilatant materials [5,6], possibly including anisotropy [16]. The main difference lies in that the rotation-rate is interpreted as ‘the rate of rotation of the sliding elements’ in the former model and as ‘the rate of rotation of principal stresses’ in the latter model. However, these kinematic models can be unified by introducing an angular velocity  $\vartheta$  [7]. Furthermore, based upon a discrete micro-analysis of the kinematics of particles in contact, this  $\vartheta$  can be alternatively interpreted as a quantity called the *averaged micro pure rotation-rate* (APR) and hence a ‘*double-slip and rotation-rate model*’ (DSR<sup>2</sup> model) was proposed [8]. The main common basis of the theories is that the deformation is postulated to occur by shear along stress/velocity characteristics, hence we may refer to them as double-shearing type kinematic models. Up to now, investigations have been carried out into some kinematic models experimentally, theoretically and numerically, which are introduced briefly as follows:

## 2.1 Experiments

Several experiments have been carried out with main aim to examine the rotation rate in the double-shearing model.

Drescher [17] carried out an experimental investigation of flow rules for granular materials by using a double-shear apparatus. In his study, optically-sensitive crushable glass particles were adopted as model granular material. By observing large shearing deformations (up to 40%) of this model granular material under circularly polarized light, the patterns of the principal stress trajectories were observed continuously and directly. These trajectories were then compared with the principal strain-increment directions, which were computed from incremental displacement fields. The experimental results showed a significant deviation between the principal axes of stress and strain-increment, i.e. non-coaxiality. In addition, Drescher [17] found that the rotation of the slip-lines differs significantly, both in magnitude and in sign, from the rotation of the principal axes of stress. He also stated that ‘..... the lines in the sliding directions can rotate dependently from the principal stress directions; this is assumed in the de Josselin de Jong rule: the constraint imposed on rotation rate in Spencer’s law is too strong’. However, further analysis on Drescher’s experimental data, by Mehrabadi and Cowin [18], showed that the de Josselin de Jong hypothesis concerning energy dissipation is not generally satisfied by these data. Furthermore, in order that all examined points should satisfy the dissipation requirement, the internal frictional angle  $\phi$  would have to be greater than or equal to  $79^\circ$ . This value for  $\phi$  is evidently far in excess of any  $\phi$ -value reported for granular materials.

Mandl et al. [19] carried out simple shear test on a layer of a granular material using a ring-shear apparatus, in which

the material underwent simple shear subject to a constant stress perpendicular to the plane of shear. In their test, very large shear strains (>1000%) were imposed. They observed that as the shear stress was increased, the principal compression axis rotated into coincidence with the principal strain-rate axis, so that both were inclined at a  $45^\circ$  angle to the shear plane. For ‘left-lateral’ shear in which the top boundary moves horizontally toward the left-hand, the principal stress axes rotated clockwise to this limiting orientation as the shear stress increased, where for ‘right-lateral’ shear, the rotation was counter-clockwise. Similar observation was reported by Savage and Lockner [20] in triaxial compression tests on a granite cylinder, in which a diagonal saw cut was inclined at an angle to major compression stress axis and confined a layer of dry sand. Savage and Lockner thought that the rotation of the principal compression axis associated with the imposed simple shear strain predicted by the Spencer [2] flow law is not in agreement with that observed by them and by others [17,19].

## 2.2 Theoretical analyses

Theoretical analyses have been carried out on the double-shearing model, the double-sliding free rotating model, and the DSR<sup>2</sup> model.

The double-shearing model assumes the rate of rotation as ‘the rate of rotation of principal stresses’. Define a *steady stress solution*, in which the stress and hence the angle  $\theta_T$  the major principal stress axis makes with the  $X$ -axis is constant or independent of time  $t$ , i.e.  $\dot{\theta}_T = \frac{d\theta_T}{dt} = 0$ . Also define a *time-dependent stress solution*, in which the stress and hence  $\theta_T$  depends on time  $t$ , i.e.  $\dot{\theta}_T \neq 0$ . Spencer [21,22] concluded that the double-shearing theory admits steady stress solutions for the plane strain deformations of simple shear and pure shear, and for compression of a circular cylinder, but these solutions are all linearly unstable. In addition, the theory yields time-dependent exact solutions for these problems in which the deformation takes place under decreasing load, which also indicates instability. The instability and the instability of the model can be used to explain the difference between the experimental data and the predicted results. Harris [23] also noted that the double-shearing equations (as well as several other models of granular material mechanics) are linearly ill-posed in the sense that small perturbations of solutions of the equations may grow exponentially. He regarded that the ill-posedness of the double-shearing model is due to the choice of the rate of rotation of principal stresses as a measure of the rate of rotation that has a property associated with a Cosserat continuum, namely, the intrinsic spin [24].

The double-sliding free-rotating model emphasizes that the sliding elements rotate freely [4]. Since the model, is indeterminate, an alternative formulation places a restriction on the model, namely the requirement of the non-negativity of the energy dissipation in each of the two slip directions, which imposes that the shear strain rate along each slip-line be non-negative. This free rotation of the sliding elements has been

regarded as equivalent to free rotation of the slip-lines by several researchers [17, 18]. In this case, Mehrabadi and Cowin [18] proved that the dissipation requirement is neither necessary nor sufficient to imply that the local energy dissipation is positive. In addition, the restriction leads to another equivalent inequalities that the rotation of slip-lines must always satisfy. Hence, it was thought that the restriction in the double-sliding free rotating model may give rise to a model inconsistent with the initial idea of ‘free’ rotation for dilatant and as well as incompressible materials [18].

The above theoretical analyses are based on classical continuum mechanics. Based upon a discrete micro-analysis of the kinematics of particles (disks) in contact, the authors [8] have recently suggested that this  $\vartheta$  can be interpreted as the *averaged micro pure rotation-rate* (APR), which is an averaged quantity generally related to *particle rotation* and *particle size* and appears to be an appropriate link between discrete micromechanics and continuum mechanics. The choice of the APR as the rotation rate leads to the ‘*double-slip and rotation-rate model*’ (DSR<sup>2</sup> model). The macro-micro mechanical analysis has shown that *the APR is a non-linear function of, among other quantities, the macro rotation-rate of the major principal axis of stress taken in the opposite sense*. It may, in general, contribute to the energy dissipation in granular materials, which leads to an actual dissipation-rate different from that described in classical continuum mechanics. A first approximation to the APR will also lead to practical kinematic theories within classical continuum mechanics, which will be briefly introduced in the next section. In addition, it has been shown that the particular requirement of energy dissipation used in the double sliding free rotating model appears to be unduly restrictive as a constitutive assumption [8]. Hence, the study appears to have solved the long-term argument on the rotation rate in kinematic theories, and found the mechanism to explain why the assumptions of the rotation rate in the double-shearing model and the double-sliding free-rotating model are both too restrictive for constitutive modeling.

### 2.3 Numerical analyses

Recently, the Distinct Element Method (DEM) has been used by the authors to examine the double-shearing model; the double-sliding free-rotating model and the ‘*double-slip and rotation-rate model*’ (DSR<sup>2</sup> model) [25,26]. This numerical technique identifies each particle separately, with its own mass, moment of inertia and contact properties. It assumes basic constitutive laws, which reduce to the Mohr-Coulomb friction law for granular materials, at interparticle contacts and provides a macroscopic/microscopic response of the particle assemblage due to incremental loading. In these analyses, a two dimensional DEM code developed by one of the authors [27,28] was used, which is in essence similar to that proposed by Cundall and Strack [29,30]. Strain rate-controlled monotonic/cyclic simple shear tests were designed to impose the incompressibility requirement and to obtain

the theoretical solution to the rotation rate in the kinematic models. The rotation rate of principal stresses and the *averaged micro pure rotation-rate* (APR), which are chosen as the rotation rate in the double-shearing model and the DSR<sup>2</sup> model respectively, were measured directly from the DEM simulations and then compared with this theoretical solution of the rotation rate. In addition, the requirement of the energy dissipation in the double-sliding free rotating model was examined through an equivalent inequality proposed by Mehrabadi and Cowin [18]. The DEM analyses have shown that the assumption used in the double-shearing model appears not to be in agreement with the DEM data, on one hand. On the other hand, the requirement of energy dissipation used in the double sliding free rotating model is generally not satisfied in the DEM simulations and appears to be unduly restrictive. However, the DSR<sup>2</sup> model can give predictions in agreement with the observations in the DEM numerical experiments [26]. The numerical analyses confirm the theoretical analyses in [8], indicating that the APR is a very important variable in kinematic models, and the DSR<sup>2</sup> model represents a successful hybrid of discrete and continuum models for non-coaxial granular materials.

The above examination works have offered good understanding of kinematic theories. However, as can be seen, these analyses require some unconventional theoretical, experimental or numerical technique to carry out, which may not be easily obtained by geo-researchers. Moreover, the exhibited aspects appear to be distant from current main topics interesting to geo-researchers. Hence, we shall in the next section propose a novel approach to examine the double-shearing type kinematic models.

## 3 Rotation of Principal Axes Method (RPAM)

In this section, after introducing some basic formulation, we shall present the Rotation of Principal Axes Method (RPAM) to examine kinematic models. The key point of the RPAM is to analyze the predicted rotation of the principal stress axes by each kinematic model, under a specially designed velocity field.

### 3.1 Basic formulation

In a plane strain Eulerian velocity field in terms of velocity components  $V_i$  (the subscript  $i=1, 2$  representing  $X$  and  $Y$  respectively), based on continuum mechanics, the components of the stress tensor  $T_{ij}$ , the deformation rate tensor  $D_{ij}$ , spin tensor  $W_{ij}$  and strain tensor  $E_{ij}$  are denoted respectively as

$$T_{ij} = \begin{bmatrix} T_{11} & T_{12} \\ T_{21} & T_{22} \end{bmatrix}; D_{ij} = \begin{bmatrix} D_{11} & D_{12} \\ D_{12} & D_{22} \end{bmatrix}; W_{ij} = \begin{bmatrix} 0 & W_{12} \\ -W_{12} & 0 \end{bmatrix} \quad (1a, b, c)$$

$$E_{ij} = \begin{bmatrix} E_{11} & E_{12} \\ E_{12} & E_{22} \end{bmatrix} = \int \begin{bmatrix} D_{11} & D_{12} \\ D_{12} & D_{22} \end{bmatrix} dt \quad (2)$$

where  $t$  is time, and  $D_{ij}$ ,  $W_{ij}$  are defined respectively by

$$D_{ij} = \frac{1}{2} \left( \frac{\partial V_i}{\partial X_j} + \frac{\partial V_j}{\partial X_i} \right); \quad W_{ij} = \frac{1}{2} \left( \frac{\partial V_i}{\partial X_j} - \frac{\partial V_j}{\partial X_i} \right) \quad (3a, b)$$

Note that, in the kinematic models concerned [1–9],  $T_{ij}$  is a symmetric tensor, i.e.  $T_{12} = T_{21}$ . Since we will discuss the possibility of choosing a Cosserat rotation rate in the kinematic models later, which may lead to an asymmetric  $T_{ij}$ , we now present general expressions so that both  $T_{12} = T_{21}$  and  $T_{12} \neq T_{21}$  are included. In addition,  $D_{ij}$  will be referred to as strain rate tensor somewhere for simplicity.

Consider a deviator stress plane in terms of  $T_\alpha$  and  $T_\beta$ , which are defined respectively by

$$T_\alpha = T_{11} - T_{22}; \quad T_\beta = T_{12} + T_{21} \quad (4a, b)$$

To describe stress paths clearly on the deviatoric stress plane, let  $\theta_T$  be the angle the major principal stress axis makes with the  $X$ -axis,

$$\tan 2\theta_T = \frac{T_{12} + T_{21}}{T_{11} - T_{22}} = \frac{T_\beta}{T_\alpha} \quad (5)$$

Note that  $\theta_T$  in Eq. (5) reduces to the same definition as used in the kinematic models concerned [1–9], in which  $T_{12} = T_{21}$ .

Turn to a deviator strain (rate) plane in terms of  $E_\alpha$  and  $E_\beta$  ( $D_\alpha$  and  $D_\beta$ ), which are defined respectively by

$$E_\alpha = E_{11} - E_{22}; \quad E_\beta = 2E_{12}; \\ D_\alpha = D_{11} - D_{22}; \quad D_\beta = 2D_{12} \quad (6a, b, c, d)$$

In order to show stress paths clearly on the deviator strain (rate) plane, let  $\theta_E$  ( $\theta_D$ ) denote the angle the major principal strain (rate) axis makes with the  $X$ -axis

$$\tan 2\theta_E = \frac{2E_{12}}{E_{11} - E_{22}} = \frac{E_\beta}{E_\alpha}; \\ \tan 2\theta_D = \frac{2D_{12}}{D_{11} - D_{22}} = \frac{D_\beta}{D_\alpha} \quad (7a, b)$$

where  $\theta_E$  ( $\theta_D$ ) is defined identically as that in the kinematic models in [1–9].

### 3.2 Designed velocity field

We now design a periodic planar Eulerian velocity field in terms of velocity components  $V_i$  (the subscript  $i = 1, 2$  representing  $X$  and  $Y$  respectively) by

$$V_1 = 2AX_2 \cos 2\omega t + AX_1 \sin 2\omega t; \quad V_2 = -AX_2 \sin 2\omega t \quad (8a, b)$$

where  $A$  is a constant in ( $\text{sec}^{-1}$ ),  $\omega$  is constant in ( $\text{rad/sec}$ ) and  $t$  is time. We shall discuss main features of this planar Eulerian velocity field below.

The deformation rate tensor  $D_{ij}$  and the spin tensor  $W_{ij}$  can be obtained from Eqs. (3) and (8) as follows

$$D_{11} = A \sin 2\omega t; \quad D_{12} = A \cos 2\omega t; \\ D_{22} = -A \sin 2\omega t; \quad W_{12} = A \cos 2\omega t \quad (9a, b, c, d)$$

Equations (2) and (9) lead to the strain tensor  $E_{ij}$ , which reads

$$E_{11} = \frac{A}{2\omega} (1 - \cos 2\omega t); \quad E_{22} = \frac{A}{2\omega} (\cos 2\omega t - 1); \\ E_{12} = \frac{A}{2\omega} \sin 2\omega t \quad (10a, b, c)$$

Equations (9)–(10) give rise to the volumetric strain (rate), denoted by  $E_v$  ( $D_v$ ), as follows

$$E_v = E_{11} + E_{22} = 0; \quad D_v = D_{11} + D_{22} = 0 \quad (11a, b)$$

Equations (11) indicate that the velocity field designed does not lead to volume change, a condition required as incompressibility in Eqs. (18a), (20a) or (26a) in Subsect. 3.3.

The deviatoric strain (rate)  $E_\alpha$  and  $E_\beta$  ( $D_\alpha$  and  $D_\beta$ ) can be derived from Eqs. (6), (9)–(10), respectively

$$E_\alpha = \frac{A}{\omega} (1 - \cos 2\omega t); \quad E_\beta = \frac{A}{\omega} \sin 2\omega t \quad (12a, b)$$

$$D_\alpha = 2A \sin 2\omega t; \quad D_\beta = 2A \cos 2\omega t \quad (12c, d)$$

Equations (12) give rise to

$$\left( E_\alpha - \frac{A}{\omega} \right)^2 + E_\beta^2 = \left( \frac{A}{\omega} \right)^2; \quad D_\alpha^2 + D_\beta^2 = 4A^2 \quad (13a, b)$$

which represents a cycle on a  $E_\alpha$ – $E_\beta$  ( $D_\alpha$ – $D_\beta$ ) plane.

In addition, the angle of principal strain (rate) ( $\theta_D$ ) deduced from the velocity field can be obtained from Eqs. (7), (9)–(10) as follows

$$\theta_E = \frac{\pi}{4} - \frac{\omega t}{2}; \quad \theta_D = \frac{\pi}{4} - \omega t \quad (14a, b)$$

Equations (12)–(14) indicate that, on the  $E_\alpha$ – $E_\beta$  ( $D_\alpha$ – $D_\beta$ ) plane, the designed velocity field represents a strain (rate) path as a circle of radius  $\frac{A}{\omega} (2A)$  characterized by a *continuous rotation of the principal strain (rate) axes*. If  $\omega = 0$  then  $\theta_E = 45^\circ$ . If  $\omega < 0$  then, according to Eq. (14a),  $\theta_E > 45^\circ$  and as a result the rotation of  $\theta_E$  is counter-clockwise. If  $\omega > 0$  then  $\theta_E$  rotates clockwise as indicated in Fig. 1. Note that, in order to illustrate Eq. (7a) clearly,  $\theta_E$  is plotted by choosing  $\theta_E \neq 45^\circ$  in Fig. 1. Moreover,  $\theta_D$  changes with  $\omega t$  while  $\theta_E$  with  $\frac{\omega t}{2}$ , which shows that the principal strain rate axes rotate at an angular rate twice that of principal strain axes, linearly with time  $t$ .

At  $t = 0$ , Eqs. (9)–(10) and (14) lead to

$$E_{11} = E_{22} = E_{12} = 0; \quad D_{11} = D_{22} = 0; \\ D_{12} = A = W_{12}; \quad \theta_D = \theta_E = \frac{\pi}{4} \quad (15a, b, c, d)$$

In summary, the incompressibility and a continuous rotation of the principal strain (rate) axes are main features of the velocity field designed. In the next subsection, we shall introduce some kinematic models that are to be analysed for this type of velocity field.

### 3.3 Double-shearing type kinematic models

The kinematic models for granular material flow were developed by several researchers [1–6] with two different

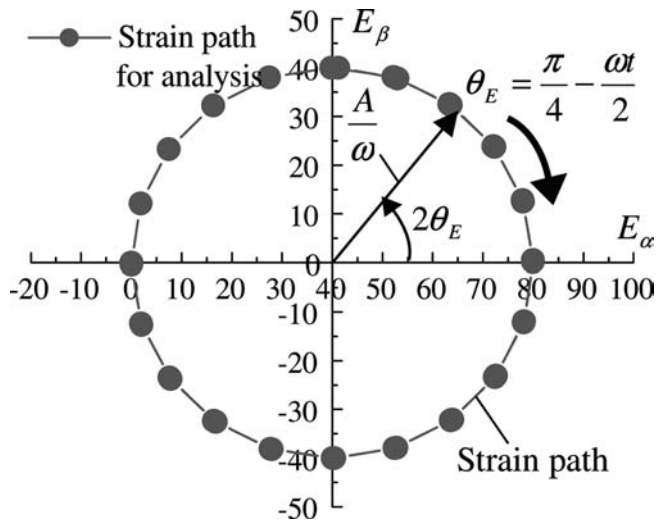


**Fig. 1** The velocity field for analyses, expressed on deviator strain plane in terms of  $E_\alpha$  and  $E_\beta$ . ( $E_\alpha = E_{11} - E_{22}$ ,  $E_\beta = 2E_{12}$ )

interpretations of the rotation rate, and can be unified by introducing an angular velocity  $\vartheta$  [7]. Recent study by the authors shows that this  $\vartheta$  can be given an alternative interpretation as a quantity called the *averaged micro pure rotation-rate* (APR) [8]. A simplified model, originally called the *simplified double-slip and rotation-rate model*, was suggested for practice by choosing a first approximation to the APR. Since this simplified model keeps all variables/quantities as well as the deformation mechanism of the double-shearing model, it may be referred to as the *revised double-shearing model*. An advantage of the rename is that several theoretical analysis methods used for the double-shearing model, e.g. Spencer [9, 21, 22] and Harris [23], will be naturally and directly applicable to any further theoretical investigation into the revised model. Since all these models postulate that the deformation occurs by shear along a pair of stress/velocity characteristics, we shall refer to them as the *double-shearing type kinematic models* herein. For completeness, we shall briefly introduce these kinematic theories by way of a unified formulation for plasticity models due to Harris [7]. This model originally results in a single derivation and presentation of the equations for the double-sliding free rotating model, the double shearing model and the plastic potential model for granular materials. The unified kinematic equations governing the velocity field are

$$(D_{11} + D_{22}) \cos\left(\frac{\nu + \lambda}{2}\right) = [(D_{11} - D_{22}) \cos 2\theta_T + 2D_{12} \sin 2\theta_T] \sin\left(\frac{\nu - \lambda}{2}\right) \quad (16a)$$

$$2(\vartheta + W_{12}) \sin\left(\frac{\nu + \lambda}{2}\right) = [(D_{11} - D_{22}) \sin 2\theta_T - 2D_{12} \cos 2\theta_T] \cos\left(\frac{\nu - \lambda}{2}\right) \quad (16b)$$

where the deformation rate tensor  $D_{ij}$  and the spin tensor  $W_{ij}$  are defined in Eqs. (3).  $\theta_T$  is the angle the major principal stress axis makes with the  $X$ -axis as defined in Eq (5). The quantities  $\nu$  and  $\lambda$  are material parameters, and  $\vartheta$  is an angular velocity which may be given a number of physical interpretations.

Firstly, by choosing  $\vartheta = \dot{\theta}_T$ ,  $\nu = \phi$ , the angle of internal friction and  $\lambda = \phi - 2\chi$  where  $\chi$  is a dilatancy parameter, Eqs. (16) become the Mehrabadi & Cowin equations [5], the double-shearing model for dilatant materials,

$$(D_{11} + D_{22}) \cos(\phi - \chi) = [(D_{11} - D_{22}) \cos 2\theta_T + 2D_{12} \sin 2\theta_T] \sin \chi \quad (17a)$$

$$2(\dot{\theta}_T + W_{12}) \sin(\phi - \chi) = [(D_{11} - D_{22}) \sin 2\theta_T - 2D_{12} \cos 2\theta_T] \cos \chi \quad (17b)$$

Note that recent studies on granular material indicate that  $\chi$  is probably not a constant and its explicit form is among our future investigation.

Equations (17) reduce to the Spencer equations [2], the double-shearing model for incompressible materials, when  $\chi = 0$ ,

$$D_{11} + D_{22} = 0; \\ 2(\dot{\theta}_T + W_{12}) \sin \phi = (D_{11} - D_{22}) \sin 2\theta_T - 2D_{12} \cos 2\theta_T \quad (18a, b)$$

Secondly, by choosing  $\vartheta$  as an indeterminate material rotation-rate;  $\nu = \phi$ ; and  $\lambda = \phi - 2\chi$ ; Eqs. (16) become one formulation of the double-sliding free-rotating model for dilatant materials

$$(D_{11} + D_{22}) \cos(\phi - \chi) = [(D_{11} - D_{22}) \cos 2\theta_T + 2D_{12} \sin 2\theta_T] \sin \chi \quad (19a)$$

$$2(\vartheta + W_{12}) \sin(\phi - \chi) = [(D_{11} - D_{22}) \sin 2\theta_T - 2D_{12} \cos 2\theta_T] \cos \chi \quad (19b)$$

The model was originally proposed for incompressible materials, for which  $\chi = 0$ , thus giving

$$D_{11} + D_{22} = 0; \\ 2(\vartheta + W_{12}) \sin \phi = (D_{11} - D_{22}) \sin 2\theta_T - 2D_{12} \cos 2\theta_T \quad (20a, b)$$

Since  $\vartheta$ , and hence the double-sliding free-rotating model, is indeterminate, an alternative formulation places a restriction on the model, namely the requirement of the non-negativity of the energy dissipation in each of the two slip directions [4]. By denoting  $a$  and  $b$  the shear strain-rates along the  $S_1$  and  $S_2$  slip-lines that are inclined at angles  $\theta_T \mp \pi/4 \mp \phi/2$  to the  $X$ -axis respectively, de Josseling de Jong [4] stipulates two inequalities that  $a$  and  $b$  must satisfy,

$$a \geq 0, \quad b \geq 0 \quad (21a, b)$$

By introducing the deviation angle  $i$  between the principal directions of the stress and deformation rate tensors by

$$i = \theta_D - \theta_T \quad (22)$$

de Josseling de Jong [4] proves that inequalities (21) lead to a requirement that this deviation angle obeys

$$-\frac{\phi}{2} \leq i \leq +\frac{\phi}{2} \quad (23)$$

Finally, we turn to our most recent extension of Eqs. (16). To meet the need for a simple non-coaxial model for granular materials for current and practical use in geotechnical engineering, a revised double-shearing model was suggested with a first approximation to the APR [8]. The approximation to the APR was given by the authors in the original paper (see Eq. (37) in [8]), and the reader can refer to [8] for the detail. We shall give this approximation here directly but in a different way. In fact, the approximation (Eq. (37) in [8]) can be in essence rewritten here as

$$\vartheta = -\frac{h+1}{h}W_{12} - \frac{\dot{\theta}_T}{h} \quad (24)$$

where  $h$  is a dimensionless quantity which generally is non-negative and depends upon the *mean stress* and the *particle size distribution* [8]. It is easy to prove that Eq. (24) is equivalent to the original approximation in [8]. Similarly, by choosing  $\nu = \phi$ ,  $\lambda = \phi - 2\chi$  and Eq. (24), the revised double-shearing model for dilatant materials is expressed by

$$(D_{11} + D_{22}) \cos(\phi - \chi) = [(D_{11} - D_{22}) \cos 2\theta_T + 2D_{12} \sin 2\theta_T] \sin \chi \quad (25a)$$

$$-\frac{2}{h}(\dot{\theta}_T + W_{12}) \sin(\phi - \chi) = [(D_{11} - D_{22}) \sin 2\theta_T - 2D_{12} \cos 2\theta_T] \cos \chi \quad (25b)$$

For incompressible materials in which  $\chi = 0$ , the model becomes

$$D_{11} + D_{22} = 0; \\ -\frac{2}{h}(\dot{\theta}_T + W_{12}) \sin \phi = (D_{11} - D_{22}) \sin 2\theta_T - 2D_{12} \cos 2\theta_T \quad (26a, b)$$

The revised double-shearing model includes several features: (a) the non-coaxial behaviour of granular materials [10] can be captured by this model provided that  $h$  is of a finite value; (b) Eqs. (25.b) and (26.b) are still frame-indifferent, which satisfies a basic requirement for constitutive modelling; (c) Eq. (24) satisfies a relationship between the APR and  $\dot{\theta}_T$  required by the theoretical analysis [8], i.e. the APR is a non-linear function of, among other quantities, the macro rotation-rate of the major principal axis of stress  $\dot{\theta}_T$  taken in the opposite sense; (d) when  $h = -1$ , even though this is against the micro-analysis in [8], the model reduces to the double-shearing model; when  $h$  is indeterminate, the model is in essence similar to the double-sliding free rotating model.

Note that in the aforementioned kinematic models, the equations governing volumetric strain rate, e.g. Eqs. (17.a), (19.a) and (25.a) for a dilatant material, are identical. However, the other equation in each model is different.

Since the velocity field designed leads to the requirement of incompressibility, see Eqs. (11), we shall next investigate the models for incompressible materials under the velocity field.

### 3.4 Kinematic models under the velocity field

The equation governing volumetric strain is naturally satisfied by Eq. (11.b), and hence omitted in this subsection. Focus will be put on the other equation in each model.

Firstly, we substitute Eqs. (9) into Eq. (18.b), the double-shearing model for incompressible granular material, giving

$$(\dot{\theta}_T + A \cos 2\omega t) \sin \phi = A \sin 2\omega t \sin 2\theta_T - A \cos 2\omega t \cos 2\theta_T \quad (27)$$

Equation (27) can be rewritten into

$$\dot{\theta}_T = -\frac{A}{\sin \phi} \cos 2(\omega t + \theta_T) - A \cos 2\omega t = f_1(\theta_T, t) \quad (28)$$

which is a non-linear firstorder differential equation of  $\theta_T$ .

Secondly, substitute Eqs. (9) into Eq. (26.b), the revised double-shearing model for incompressible granular material, leading to

$$(\dot{\theta}_T + A \cos 2\omega t) \frac{\sin \phi}{h} = -A \sin 2\omega t \sin 2\theta_T + A \cos 2\omega t \cos 2\theta_T \quad (29)$$

Arranging Eq. (29) leads to

$$\dot{\theta}_T = \frac{Ah}{\sin \phi} \cos 2(\omega t + \theta_T) - A \cos 2\omega t = f_2(\theta_T, t) \quad (30)$$

which again is a non-linear first-order differential equation of  $\theta_T$ .

Equations (27)–(30) show that the kinematic model becomes a non-linear firstorder differential equation of  $\theta_T$  under the designed velocity field. Since it is difficult or impossible to find an explicit analytical solution to this differential equation, the *Euler's* numerical method will be adopted to find an approximate solution. The detail on this method can be found in any textbooks on *Engineering Mathematics*. For the clearness, we shall introduce this method through a nonlinear function  $f(\theta_T, t)$ . Given a first-order differential equation, similar to Eq. (28) or (30), as follows

$$\frac{d\theta_T}{dt} = f(\theta_T, t) \text{ with } \theta_T(t_0) = \theta_T^0 \quad (31)$$

the solution to  $\theta_T(t)$  can be obtained by using the formula

$$\theta_T(t^{j+1}) = \theta_T(t^j) + f[\theta_T(t^j), t^j] \Delta t \quad (32)$$

where  $t^{j+1} = t^j + \Delta t$  and  $j = 0, 1, 2, \dots, n$ . The smaller is the value of incremental time  $\Delta t$ , the better is the accuracy of the *Euler's* method. So, the  $\theta_T$  predicted by the double-shearing model or the revised double-shearing model can be obtained under the velocity field.

Finally, the  $i$  required in Eq. (23), can be regarded as a way controlling the  $\theta_T$  of the double-sliding free-rotating model under the designed velocity field.

Hence  $\theta_T$  of each double-shearing type model can be analysed. Since the velocity field represents a continuous rotation of principal strain or strain rate axes, we shall refer to this examination method as the Rotation of Principal Axes Method (RPAM). In addition, the rotation of the

principal axes in monotonic/cyclic loading has been evidently observed and greatly emphasized in the geotechnical community [31, 32]. Therefore, the RPAM can examine the kinematic models in a way interesting to geo-researchers. In the next section, the RPAM will be used to analyse the main features of the double-shearing type models, mainly for a granular material of internal frictional angle  $35^\circ$ .

#### 4 Features of double-shearing type models by RPAM

The Rotation of Principal Axes Method (RPAM) will be used to investigate  $\theta_T(t)$  the angle the major principal stress axis makes with the  $X$ -axis for the double-shearing type kinematic model under the designed velocity field. In the analyses, the parameters controlling the velocity field are chosen as follows:  $A = 0.04\pi$  ( $\text{sec}^{-1}$ ),  $\omega = 0.1\pi$ . This choice leads to a clockwise rotation of strain path on the deviator strain  $E_\alpha - E_\beta$  plane with the maximum value of  $E_\alpha$  or  $E_\beta$  as 40%, as illustrated in Fig. 1. Note that, in order to illustrate Eq. (7a) clearly,  $\theta_E$  is plotted by choosing  $\theta_E \neq 45^\circ$  in Fig. 1. In addition, an incremental time  $\Delta t = 2.0 \times 10^{-5}$  is used to obtain  $\theta_T(t)$  in a duration of  $t = 0 \sim 20$  seconds (s), which corresponds to a rotation of principal strain rate axes  $\theta_D$  around  $360^\circ$ . We shall first analyse the accuracy of approximate solutions, and then main features of the double-shearing type kinematic models. Finally, we shall discuss the possibility of choosing a Cosserat rotation rate in kinematic theories and the way to determine parameter  $h$  in the revised double-shearing model.

##### 4.1 Accuracy of solutions

Our several trial calculations show that the choice of  $\Delta t = 2.0 \times 10^{-5}$  is small enough to obtain a highly accurate approximate solution. Take a numerical solution to the double-shearing model for a material of internal frictional angle  $\phi = 35^\circ$  as an example. Table 1 presents the calculated  $\theta_T$  at  $t = 3$  s by the Euler's method using different  $\Delta t$ , from  $2.0 \times 10^{-2}$  to  $2.0 \times 10^{-7}$  s. In this example the initial principal stress angle  $\theta_T^0$  is taken to be  $45^\circ$ . Table 1 shows that  $\theta_T$  is around  $52^\circ$  at  $t = 3$  s. When  $\Delta t \leq 2.0 \times 10^{-3}$ , the difference in  $\Delta t$  leads to little difference in  $\theta_T$ . Assume that  $\Delta t = 2.0 \times 10^{-7}$  gives rise to an accurate solution. Table 1 shows that the choice of  $\Delta t = 2.0 \times 10^{-5}$  in this study leads to a very small relative error of  $2.1 \times 10^{-4}\%$ . Hence, we may think that the approximate solution to  $\theta_T$  of each model below is reliable.

##### 4.2 The double-shearing model

The double-shearing model assumes the rate of rotation in kinematic theories as the rate of rotation of principal stresses. Figure 2(a) provides variations of principal stress angle  $\theta_T$  predicted by the model under the velocity field concerned, for a granular material of internal friction angle  $\phi = 35^\circ$ .

Considering that  $t = 0 \Rightarrow D_{12} \neq 0$ ,  $\theta_D = \frac{\pi}{4}$ ,  $\theta_T =$  undetermined, see Eqs. (15), five different values of initial principal stress angle  $\theta_T^0$  are selected around  $45^\circ$ , from  $0^\circ$  to  $90^\circ$ . This range of  $\theta_T^0$  should be able to cover any reasonable choice of  $\theta_T^0$ . In addition, in Fig. 2(a), the  $\theta_T$  predicted by the coaxial model is provided, which corresponds to the coincidence of the principal stress tensor and the principal deformation-rate tensor, i.e.  $\theta_T = \theta_D$ . Hence, the vertical difference between  $\theta_T$  predicted by the coaxial model and the kinematic model in Fig. 2(a) (as well as in the other figures below) is the deviation angle  $i$  between the principal directions of the stress and deformation rate tensors. Figure 2(a) shows that different  $\theta_T^0$  leads to different variation of  $\theta_T$ . In all cases, the magnitude of the predicted  $\theta_T$  varies less than  $100^\circ$  although  $\theta_D$  changes from  $45^\circ$  to  $-325^\circ$ . This indicates that the double-shearing model appears to predict a very 'delayed' rotation of the principal stress axes to the rotation of principal strain rate axes. In addition, Fig. 2(a) shows that the predicted  $\theta_T$  continuously increases but with oscillations ('waving') that exhibit an amplitude range as large as  $\pm 40^\circ$ . To further investigate the main features of the model, Fig. 2(b) present variations of  $\theta_T$  predicted by the model for materials of different  $\phi$ , from  $1^\circ$  to  $90^\circ$  for clearness, by using  $\theta_T^0 = 45^\circ$ . Figure 2(b) shows two different kinds of variation of  $\theta_T$ . When  $\phi \geq 30^\circ$ , the double-shearing model still predicts oscillations and a 'very delayed' rotation of  $\theta_T$ . When  $\phi \leq 20^\circ$ , the predicted  $\theta_T$  follows  $\theta_D$  in a stable 'delayed' manner, i.e. with a constant deviation angle  $i$  or with a slightly oscillating  $i$ . The smaller is  $\phi$ , the smaller is  $i$ . This seems to indicate that the double-shearing model appears to be able to give a qualitatively acceptable prediction of  $\theta_T$  for a material of small  $\phi$ . However, further examination in Fig. 2(b) shows that the predicted magnitude of  $i$  is larger than  $90^\circ$  in the latter case, with a tendency that  $\phi \rightarrow 0^\circ \Rightarrow i \rightarrow -90^\circ$ . This tendency is consistent with one feature of Eq. (27). Indeed, when  $\phi = 0^\circ$ , Eq. (27) gives rise to a set of solutions as follows

$$\theta_T = (2n - 1)\frac{\pi}{4} - \omega t, \quad n = 0, \pm 1, \pm 2, \pm 3, \dots \quad (33)$$

Considering Eq. (15.d), one acceptable solution among Eq. (33) is  $\theta_T = -\frac{\pi}{4} - \omega t$ , which leads to  $i = -90^\circ$ , the limit case shown in Fig. 2(b). Note that internal friction angle of real granular materials is usually between  $30^\circ \sim 40^\circ$ , which is out of the range for a stable 'delayed' prediction of  $\theta_T$  by the model.

Hence, the results obtained by RPAM in Fig. 2 show that the double-shearing model tends to predict a very 'delayed' rotation of the principal stress axis to the rotation of principal strain rate axes for granular materials. The reason for this large prediction may attribute to the fact that the model stipulates the rotation-rates as 'the rate of rotation of principal stresses'. As shown by the theoretical analyses by Spencer [21, 22], the double-shearing theory admits steady stress solutions, which are all linearly unstable. In addition, the theory also yields time-dependent exact and instable solutions.

**Table 1** Calculated angle of major principal stress  $\theta_T$  using different incremental time  $\Delta t$ : the double-shearing model, initial principal stress angle  $\theta_T^0 = 45^\circ$ , angle of internal friction  $\phi = 35^\circ$

$\Delta t$ (s)	$2.0 \times 10^{-2}$	$2.0 \times 10^{-3}$	$2.0 \times 10^{-4}$	$2.0 \times 10^{-5}$	$2.0 \times 10^{-6}$	$2.0 \times 10^{-7}$
$\theta_T$ at $t = 3$ s (degree)	52.020569	52.119651	52.129535	52.130523	52.130622	52.130632
Relative error (%)	0.211129	0.021064	0.002104	$2.1 \times 10^{-4}$	$1.9 \times 10^{-5}$	0

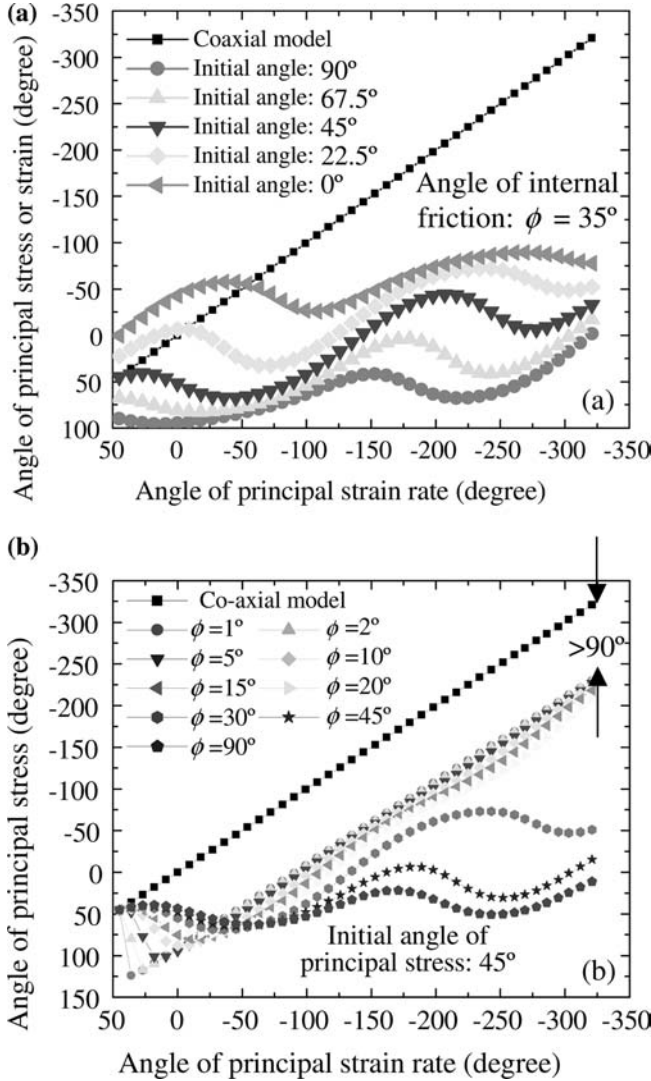


**Fig. 2** Variations of principal stress angle, predicted by the double-shearing model using different initial principal stress angle (a), and different angle of internal friction (b)

#### 4.3 The double-sliding free-rotating model

The double-sliding free-rotating model considers the rate of rotation as an indeterminate material characteristic. In addition, the model adopts Eq. (21) as an alternative restriction. This requirement does not result in a specific value of the deviation angle  $i$  between the principal stress and strain-rate tensors. Instead, it imposes a requirement for the varying range of  $i$  by inequality (23) under any condition, which must

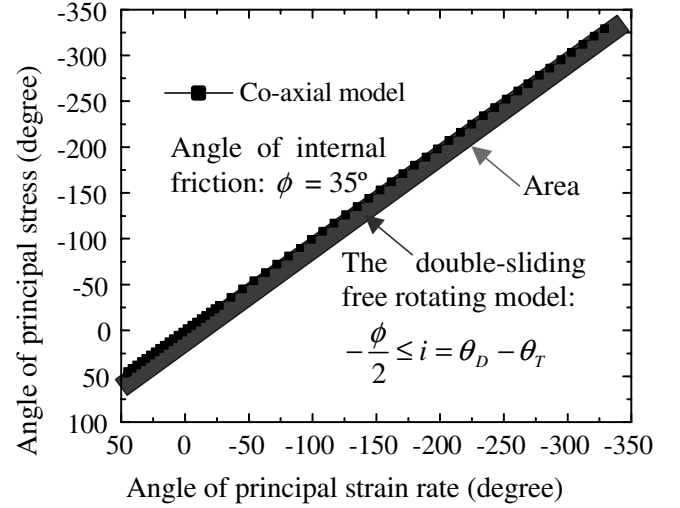


**Fig. 3** Variations of principal stress angle, predicted by the double-sliding free-rotating model

naturally include the designed velocity field. Figure 3 illustrates variations of principal stress angle  $\theta_T$ , predicted by the double-sliding free-rotating model, for a granular material of internal friction angle  $\phi = 35^\circ$ . Since inequality (23) gives a variation range, it can be plotted as area in Fig. 3. Mathematically, there are infinite curves existing in this area. Hence, Fig. 3 shows that the model may predict infinite variations of  $\theta_T$ , instead of a specific variation of  $\theta_T$ , under the designed velocity field. In this sense, the model is still indeterminate.

#### 4.4 The revised double-shearing model

The revised double-shearing model retains all variables/quantities and the deformation mechanism of the double-shearing model. In addition, it chooses the rotation rate by Eq. (24), in which a model parameter  $h$  is introduced. Figure 4(a) provides variations of principal stress angle  $\theta_T$  predicted by the model for a granular material of internal friction angle  $\phi = 35^\circ$ . In the analysis,  $h = 2.0$  is used as an example. Due to the same reason as in the analysis of the double-shearing model, different values of initial principal stress angle  $\theta_T^0$  are still chosen around  $45^\circ$ , with a range of  $\pm 45^\circ$ . Figure 4(a) shows that different  $\theta_T^0$  leads to different variation of  $\theta_T$  until total rotation of the principal strain rate axes  $|\theta_D - \theta_D^0|$  is up to  $75^\circ$ . Note that this value of  $|\theta_D - \theta_D^0|$  corresponds to the point at which  $\theta_D = -30^\circ$  in Fig. 4(a). This indicates that  $\theta_T^0$  evidently affects the initial variation of  $\theta_T$  in the revised double-shearing model, while it affects whole variation of



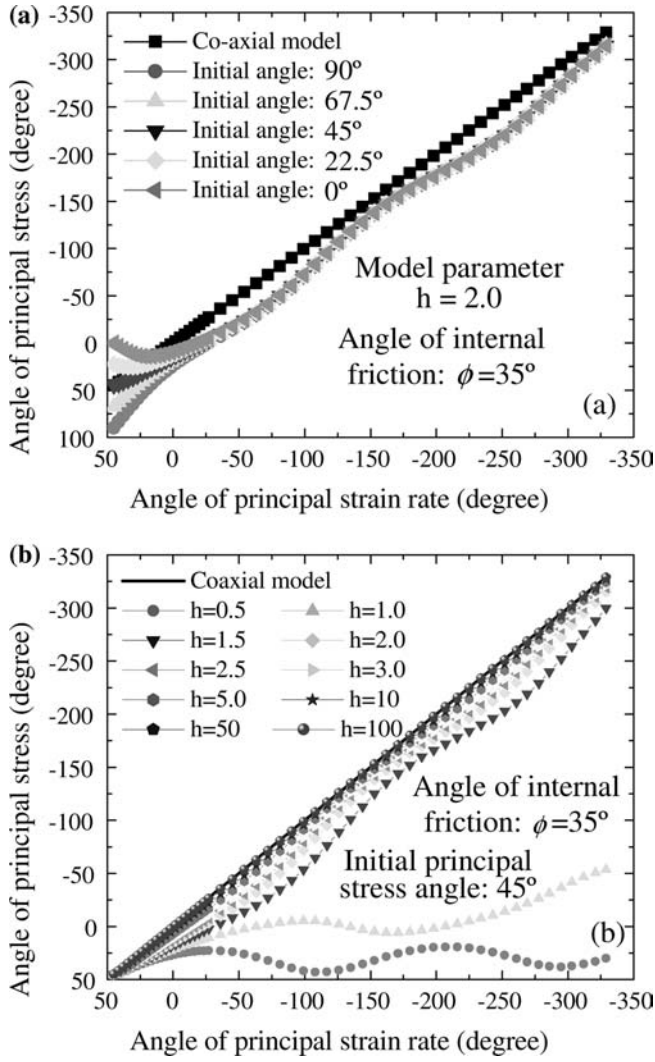


**Fig. 4** Variations of principal stress angle, predicted by the revised double-shearing model using different initial principal stress angle (a), and different value of parameter  $h$  (b)

$\theta_T$  in the double-shearing model. Then, when  $|\theta_D - \theta_D^0|$  is larger than  $75^\circ$  ( $\theta_D < -30^\circ$  in the figure), the predicted  $\theta_T$  in all cases follows  $\theta_D$  in an identical, stable ‘delayed’ way. The predicted deviation angle  $i$  between the principal directions of the stress and deformation rate tensors is about  $-25^\circ$ .

In order to further understand the main features of the model, Fig. 4(b) presents variations of  $\theta_T$  predicted by the model for materials of  $\phi = 35^\circ$  but different values of  $h$ . Again,  $\theta_T^0 = 45^\circ$  is used in the analyses. Neglect the initial part of variation of  $\theta_T$ , Fig. 4(b) shows that when  $h \leq 1.0$ , the model predicts a very oscillating and very ‘delayed’ prediction of  $\theta_T$  in a way similar to the double-shearing model. When  $h \geq 1.5$ , the predicted  $\theta_T$  follows the  $\theta_D$  in a stable ‘delayed’ manner, i.e. with a slightly oscillating or a nearly constant  $i$ . In addition, this  $i$  falls between  $0^\circ$  and  $-45^\circ$ . The larger is  $h$ , the smaller is magnitude of  $i$ , with a tendency that  $|i| \rightarrow 0$  at large  $h$ . The observations in Fig. 4 show that the revised double-shearing model appears to be able to

give a prediction of  $\theta_T$  in a stable ‘delayed’ way with different magnitude of  $i$ , provided that the value of  $h$  is carefully selected. We will discuss how to choose  $h$ , after presenting a discussion in the next subsection on the choice of a Cosserat rotation rate in kinematic theories.

#### 4.5 Discussion on choice of a Cosserat rotation rate

Based on the theoretical and numerical observations that the *averaged micro pure rotation-rate* (APR) represents the rotation rate in the kinematic theories [8,25,26], a hyperbolic, well-posed model for the flow of granular materials is being established in association with a Cosserat continuum [24]. This is a good try to combine kinematic theories for the granular flow with two key Cosserat concepts, namely, an intrinsic spin and an asymmetric stress tensor. In the model, a continuum rate of rotation phenomenon is assumed to be existent and distinct from that of the anti-symmetric part of the velocity gradient tensor, i.e. spin tensor  $W_{ij}$  in Eq. (3.b). However, the reason for elucidating the choice of  $W_{ij}$  as the rotation rate in kinematic theories is not investigated. Since Cosserate rotation rate has been traditionally chosen as  $W_{ij}$  by several researchers in strain localization simulations [33,35] as well as rapid flow [36], we shall now discuss the possibility of choosing  $W_{ij}$  as the rotation rate in kinematic theories, i.e.  $\vartheta = W_{12}$  in Eqs. (16), by the RPAM. A model of such a choice is referred to as a Cosserat-type double-shearing model in this study.

For simplicity, adopting the same simplification procedure directly as used for Eq. (16)–(18), leads to the Cosserat-type double-shearing model for incompressible materials,

$$D_{11} + D_{22} = 0;$$

$$4W_{12} \sin \phi = (D_{11} - D_{22}) \sin 2\theta_T - 2D_{12} \cos 2\theta_T \quad (34a, b)$$

Substituting Eqs. (9) into Eq. (34.b), gives rise to

$$2A \cos 2\omega t \sin \phi = A \sin 2\omega t \sin 2\theta_T - A \cos 2\omega t \cos 2\theta_T \quad (35)$$

An explicit solution to Eq. (35) may be obtained by

$$\theta_T = \frac{1}{2} \arccos(-2 \sin \phi \cos 2\omega t) - \omega t \quad (36)$$

In order to clearly describe the main features of Eq. (36), Fig. 5 provides variations of principal stress angle  $\theta_T$  numerically obtained from Eq. (36) for granular materials of  $\phi = 10^\circ, 20^\circ, 30^\circ$  respectively. Figure 5 shows that the  $\theta_T$  predicted by the model do not follows  $\theta_D$  in either stable ‘delayed’ or stable ‘advanced’ way to the coaxial model. For  $\phi \leq 30^\circ$  the predictions oscillate around the coaxial solution and coincide with it ( $i=0$ ) when total rotation of the principal strain rate axes  $|\theta_D - \theta_D^0| = 45^\circ, 135^\circ, 225^\circ$  and  $315^\circ$ , where  $\theta_D^0$  represents  $\theta_D$  at  $t = 0$  and its value is given in Eq. (15b). This shows that  $i = 0$  occurs at  $\theta_D = 90^\circ, 180^\circ, 270^\circ$  and  $360^\circ$ . It can be seen from Eq. (7b) that these points correspond to  $D_{12} = 0$  (not  $E_{12}$ ). At this time, from Eqs. (9b) and (10), we obtain

$$E_{11} = -E_{22} = E_{12} = A/2\omega, \text{ at } i = 0 \quad (37)$$

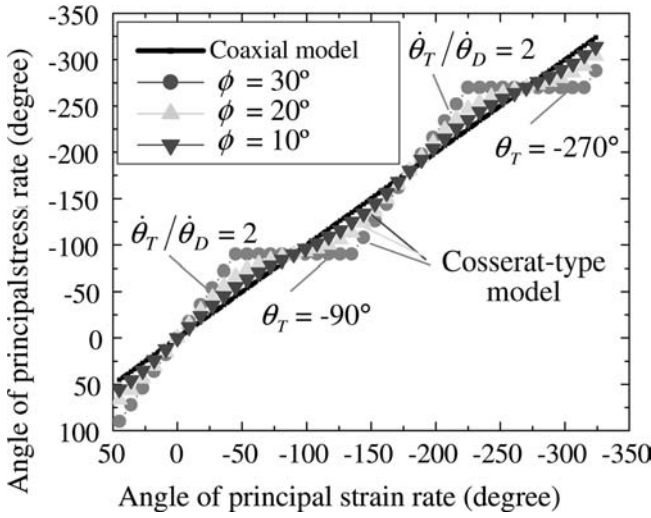


**Fig. 5** Variations of principal stress angle, predicted by a Cosserat-type double-shearing model for granular materials of different angle of internal friction  $\phi$

Interestingly the solution for  $\phi = 30^\circ$  is piecewise linear with ranges of  $\theta_D$  over  $\theta_T$  which is constant, i.e.  $\theta_T = \text{ct}$  ( $-90^\circ$  and  $-270^\circ$  in the figure) or  $\dot{\theta}_T / \dot{\theta}_D = 2$ . This tendency is consistent with the main feature of Eq. (36). Substituting  $\phi = 30^\circ$  into Eq. (36) leads to

$$\theta_T = \frac{1}{2} \arccos(-\cos 2\omega t) - \omega t \quad (38)$$

which gives rise to two sets of solutions

$$\theta_T = (2n + 1) \frac{\pi}{2}, \quad n = 0, \pm 1, \pm 2, \pm 3, \dots \quad (39a)$$

$$\theta_T = (2n + 1) \frac{\pi}{2} - 2\omega t, \quad n = 0, \pm 1, \pm 2, \pm 3, \dots \quad (39b)$$

Note that the set of solutions in Eq. (39b) can be rewritten as

$$\theta_T = (2n + 1) \frac{\pi}{2} - 2\omega t = n\pi + 2 \left( \frac{\pi}{4} - \omega t \right) = n\pi + 2\theta_D \quad (40)$$

It is easy to see that the solutions in Eq. (39a) include  $\theta_T = -90^\circ$  and  $\theta_T = -270^\circ$ , while the solutions in Eq. (40) give rise to  $\dot{\theta}_T / \dot{\theta}_D = 2$ , which are the cases shown in Fig. 5.

Figure 5 indicates that the averaged deviation angle  $i$  between principal stress and strain rate tends to be zero, at  $t \rightarrow \infty$  or at each full period of  $180^\circ$ . In addition, the smaller value of  $\phi$ , such as  $\phi = 10^\circ$ , leads to a less varying range of  $\theta_T$  about the coaxial model prediction.

Note that Eq. (36) is meaningful only when  $\phi \leq 30^\circ$ . This is because any value of  $\phi$  among  $90^\circ > \phi > 30^\circ$  may lead to the magnitude in the bracket larger than  $\pm 1.0$ , which is out of the limit required by function ‘arccos’ in Eq. (36). Considering that: (i) granular materials are usually of  $\phi$  between  $30^\circ \sim 40^\circ$ , i.e. out of the range leading to a solution to Eq. (36); (ii) no experimental data has been found to support the solutions to Eq. (36), such as Eqs. (37) and (39) yet, the investigation by the RPAM here does not support the choice of  $W_{ij}$  as the rotation rate in kinematic theories.

#### 4.6 Discussion on the parameter $h$ in the revised double-shearing model

As shown in Subsect. 4.4, the revised double-shearing model appears to be able to give a prediction of the rotation of principal stress angle  $\theta_T$  in a stable ‘delayed’ manner to the rotation of principal strain rate axes  $\theta_D$ , provided that the value of  $h$  is carefully selected. We now discuss how to determine  $h$  in order to give such a kind of predictions, by using the RPAM.

We consider the same velocity field as used above, but carry out calculations with total rotation of the principal strain rate axes  $|\theta_D - \theta_D^0| > 720^\circ$  in order to reduce possible calculation error. Four steps are used for the target. Firstly, for a given value of internal friction angle  $\phi$ , choose different  $h$  by which a stable ‘delayed’ variation of  $\theta_T$  can be obtained by the RPAM. Secondly, calculate the averaged deviation angle  $i$  between the principal directions of the stress and deformation rate tensors during  $720^\circ \geq |\theta_D - \theta_D^0| \geq 120^\circ$ . The neglect of the data within  $\theta_D < 120^\circ$  comes from the fact that initial principal stress angle  $\theta_T^0$  is selected as  $45^\circ$  in each case for simplicity and hence its effect on the initial variation of  $\theta_T$  must be avoided in the determination of the averaged  $i$ . Then, repeat the first and second steps for different  $\phi$ . Finally, a relationship can be obtained between  $\phi$ ,  $h$  and the averaged  $i$ . Figure 6 presents the relationship between  $\phi$  and  $h$ , required by the revised double-shearing model in predicting different averaged  $i(\pm 1^\circ)$ . Fig. 6 shows that for a given averaged  $i(\pm 1^\circ)$ , the value of  $h$  increases with the increasing of  $\phi$ . For a given  $\phi$ , the averaged  $i$  decreases with the increasing of  $h$ . A slightly non-linear relationship appears to stand between  $\phi$  and  $h$  for each  $i(\pm 1^\circ)$ . In addition, for a given  $\phi$ , the smaller is the  $i(\pm 1^\circ)$  considered, the larger is the range of  $\Delta h$  that is resulted from the choice of  $(\pm 1^\circ)$  for  $i$ . It is known that both  $\phi$  and  $i$  can be measured through

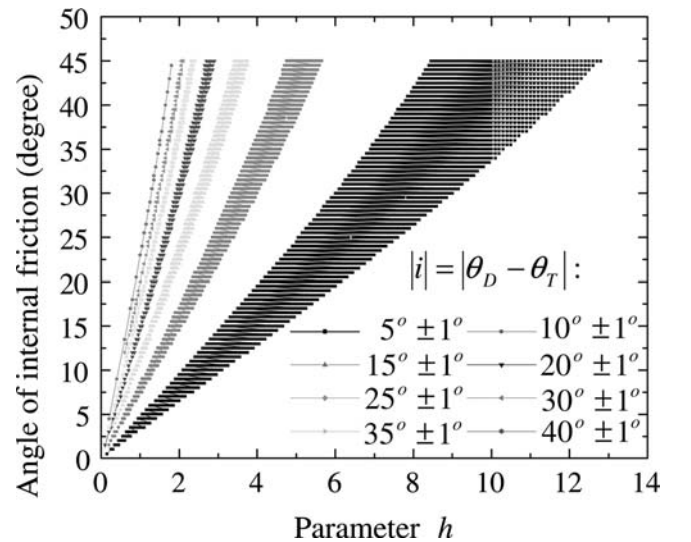


**Fig. 6** The relationship between internal frictional angle and parameter  $h$ , required by the revised double-shearing model in predicting several possible deviations between principal stress and strain rate tensors

experiments in geo-lab for a given material, such as the Fig. 9 in [37]. Hence, Fig. 6 provides an efficient way to determine parameter  $h$  in the revised double-shearing model, which can be regarded as another advantage of the proposed RPAM.

## 5 Conclusion

This paper presents a novel method, referred to as the Rotation of Principal Axes Method (RPAM), to examine the double-shearing type kinematic models for granular materials. The study is of theoretical and practical importance since the kinematic models are physically established in a simple formulation and can capture one of most complicated behaviours of granular materials, i.e. non-coaxiality. The main features of method are: (a) it is based on a planar velocity field that satisfies incompressibility condition and shows a strain (rate) path as a cycle on a deviator strain (rate) plane; (b) the Euler's numerical method is usually used in the RPAM to obtain the rotation of principal stresses  $\theta_T$ ; and (c) the examined aspect is one of most interesting and important topics in geomechanics. It is concluded from the study that:

(1) The RPAM can be used as a criterion to examine the double-shearing type theories for granular materials. In addition, it can be used to investigate other possible choice of the rotation rate in kinematic theories, and provide an efficient way to determine model parameter  $h$  in the revised double-shearing model.

(2) The application of the RPAM shows that the double-shearing model tends to predict a very 'delayed'  $\theta_T$  in a much evidently oscillating ('waving') way to the rotation of principal strain rate axes  $\theta_D$ . The double-sliding free-rotating model provides an infinite and indeterminate 'delayed' variations of  $\theta_T$ . The revised double-shearing model appears to be able to give a prediction of stable 'delayed'  $\theta_T$  with different magnitude of the deviation angle  $i$  between the principal stress and strain-rate tensors ( $0^\circ \sim 45^\circ$ ).

(3) The choice of the rigid spin tensor as the rotation rate may lead to a kinematic model that can only be able to give predictions of  $\theta_T$  for granular materials of internal frictional angle  $\phi \leq 30^\circ$ . In addition, the predicted  $\theta_T$  undergoes in a manner changing regularly and periodically between stable 'delayed' and stable 'advanced' way to  $\theta_D$ .

The Distinct Element Method [27–30] as well as plane strain experiments [34] can be used to simulate the designed velocity field and measure  $i$  for real granular materials. Together with the RPAM presented in this paper, a full evaluation on the kinematic models, including the DSR<sup>2</sup> model, can be achieved in a way familiar and attractive to geo-researchers. These works are now under way.

**Acknowledgements** The work reported here was funded by EPSRC grant with number GR/R85792/01. The authors thank the EPSRC for the financial support of the first author during his post-doctoral research on this study. Comments by the referees, and by Prof. Stefan Luding, TUDelft, The Netherlands, are also appreciated.

## References

- De Josselin de Jong, G.: The undefiniteness in kinematics for friction materials. Proc. Conf. Earth Pressure Problem, Brussels I, 1958, pp. 55–70
- Spencer, A.J.M.: A theory of the kinematics of ideal soils under planar strain conditions. J. Mech. Phys. Solids **12**, 337–351 (1964)
- Mandel, J.: Sur les lignes de glissement et le calcul des déplacements dans la déformation plastique. C.r.hebd. Séanc. Acad. Sci. Paris **223**, 1272–1273 (1947)
- De Josselin de Jong, G.: The double sliding, free rotating model for granular assemblies. Géotechnique **21**(3), 155–162 (1971)
- Mehrabadi, M.M., Cowin, S.C.: Initial planar deformation of dilatant granular materials. J. Mech. Phys. Solids **26**, 269–284 (1978)
- Anand, L.: Plane deformation of granular materials. J. Mech. Phys. Solids **31**, 105–122 (1983)
- Harris, D.: A unified formulation for plasticity models of granular and other materials. Proc. R. Soc. Lond. **A450**, 37–49 (1995)
- Jiang, M.J., Harris, D., Yu, H-S: Kinematic models for non-coaxial granular materials: Part I, theories. Int. J. for Numer. And Analyt. Methods in Geomech. **29**(7), 661–679 (2005)
- Spencer, A.J.M.: Deformation of ideal granular materials, Mechanics of Solids: the Rodney Hill Anniversary Volume, Pergamon Press, Oxford, 1982, pp. 607–652
- Gutierrez, M., Ishihara, K.: Non-coaxiality and energy dissipation in granular materials. Soils and Foundations **40**(2), 49–59 (2000)
- Li, X.S., Dafalias, Y.F.: A constitutive framework for anisotropic sand including non-proportional loading. Géotechnique **54**(1), 41–55 (2004)
- Kolymbas, D.: An outline of hypoplasticity. Archive of Appl. Mech. **61**, 143–151 (1991)
- Pande, G.N., Sharma, K.G.: A multi-laminate model of clays: a numerical study of the influence of rotation of the principal stress axes. Int. J. Num. Anal. Meth. Geomech. **7**, 397–418 (1983)
- Iai, S., Matsunaga, Y., Kameoka, T.: Strain space plasticity model for cyclic mobility. Soils and Foundations **32**(2), 1–15 (1992)
- Collins, I.F.: Plane strain characteristics theory for soils and granular materials with density dependent yield criteria. J. Mech. Phys. Solids **38**(1), 1–25 (1990)
- Nemat-Nasser, S.: A micromechanically-based constitutive model for frictional deformation of granular materials. J. Mech. Phys. Solids **48**, 1541–1563 (2000)
- Drescher, A.: An experimental investigation of flow rules for granular materials using optically sensitive glass particles. Géotechnique **26**(4), 591–601 (1976)
- Mehrabadi, M.M., Cowin, S.C.: On the double-sliding free-rotating model for the deformation of granular materials. J. Mech. Phys. Solids **29**(4), 269–282 (1981)
- Mandl, G., De Jong, L.J., Maltha, A.: Shear zones in granular material: An experimental study of their structure and mechanical genesis. Rock Mech. **9**, 95–144 (1977)
- Savage, J.C., Lockner, D.C.: A test of the double-shearing model of flow for granular materials. J. Geophysical Research **102**(B6), 12287–12294 (1997)
- Spencer, A.J.M.: Instability of steady shear flow of granular materials. Acta Mechanica **64**, 77–87 (1986)
- Spencer, A.J.M.: Double-shearing theory applied to instability and strain localization in granular materials. J. Eng. Math. **45**, 55–74 (2003)
- Harris, D.: Ill- and well-posed models of granular flow. Acta Mechanica **146**, 199–225 (2001)
- Harris, D., Grekova, E.F.: A hyperbolic well-posed model for the flow of granular materials. J. Eng. Math. (2005) (in press)
- Jiang, M.J., Harris, D., Yu, H-S: Rotation-rate in the Harris kinematic equations for post-failure flow granular materials. Int. Workshop on Predict. Simul. Meth. Geomech., Athens, Greece, Oct. 14–15, 2003, pp. 129–132
- Jiang, M.J., Harris, D., Yu, H-S: Kinematic models for non-coaxial granular materials: Part II, evaluation. Int. J. Numer. And Analyt. Methods in Geomech. **29**(7), 681–707 (2005)

- 
27. Jiang, M.J., Konrad, J.M., Leroueil, S.: An efficient technique for generating homogeneous specimens for DEM studies, *Computers and Geotechnics* **30**(7), 579–597 (2003)
  28. Jiang, M.J., Leroueil, S., Konrad, J.M.: Insight into shear strength functions of unsaturated granulates by DEM analyses. *Computers and Geotechnics* **31**(6), 473–489 (2004)
  29. Cundall, P.A., Strack, O.D.L.: The distinct numerical model for granular assemblies. *Géotechnique* **29**(1), 47–65 (1979)
  30. Thornton, C.: Numerical simulation of deviatoric shear deformation of granular media. *Géotechnique* **50**(1), 43–53 (2000)
  31. Ishihara, K., Towhata, I.: Sand response to cyclic rotation of principal stress directions as induced by wave loads, *Soils and Foundations* **23**(4), 11–26 (1983)
  32. Bjerrum, L.: Geotechnical problems involved in foundations of structures in the North Sea. *Géotechnique* **23**(3), 319–358 (1973)
  33. de Borst, R.: Simulation of strain localization: a reappraisal of the Cosserate continuum, *Engineering Computations* **8**, 317–332 (1991)
  34. Joer, H.A., Lanier, J., Fahey, M.: Deformation of granular materials due to rotation of principal axes. *Géotechnique* **48**(5), 605–619 (1998)
  35. Tejchman, J.: Comparative FE-studies of shear localizations in granular bodies within a polar and non-local hypoplasticity. *Mechanics Research Communications* **31**, 341–354 (2004)
  36. Tejchman, J., Klisinski, M.: FE-studies on rapid flow of bulk solids in silos. *Granular Matter* **3**, 215–229 (2001)
  37. Gutierrez, M., Ishihara, K., Towhata, I.: Flow theory for sand during rotation of principal stress direction. *Soils and Foundations* **31**(4), 121–132 (1991)